Aerosol Science and Technology
Publication details, including instructions for authors and subscription information:
http://www.tandfonline.com/loi/uast20

Effects of Some Geometric Parameters on the Electrostatic Precipitator Efficiency at Different Operation Indexes

Chung-Liang Chang & Hsunling Bai
Published online: 30 Nov 2010.

To cite this article: Chung-Liang Chang & Hsunling Bai (2000) Effects of Some Geometric Parameters on the Electrostatic Precipitator Efficiency at Different Operation Indexes, Aerosol Science and Technology, 33:3, 228-238, DOI: 10.1080/027868200416222

To link to this article: http://dx.doi.org/10.1080/027868200416222

Aerosol Science and Technology 33:228–238 (2000)

Published by Taylor and Francis
0278-6826/00/$12.00 + .00

Effects of Some Geometric Parameters on the Electrostatic Precipitator Efficiency at Different Operation Indexes

*Chung-Liang Chang and Hsunling Bai**
INSTITUTE OF ENVIRONMENTAL ENGINEERING, NATIONAL CHIAO TUNG UNIVERSITY,
75, PO-AI ST., HSIN-CHU, 300, TAIWAN

ABSTRACT. The performance of electrostatic precipitators (ESPs) was usually obtained under different geometric parameter values and operation indexes. Hence different conclusions were made in the literature and similar improvements may not be obtained for other applications. In this paper the effects of some geometric parameters on the performance of a wire-plate ESP at different operation indexes are evaluated theoretically. The geometric design parameters include discharge wire diameter, wire-to-wire distance, and plate-to-plate spacing. And the operation indexes considered are the electric field strength, the average current density at plates, and the corona power ratio. The results show that the collection efficiency is increased with a decrease in the wire diameter under the same electric field strength. But opposite results are observed under the same average current density at plates or the same corona power ratio applying to the ESP. The optimal wire-to-wire distance and plate-to-plate spacing vary as the electric field strength is changed. On the other hand, high collection efficiencies are always obtained with decreases in the wire-to-wire distance and the plate-to-plate spacing under the same average current density at plates or the same corona power ratio.

INTRODUCTION

The wire-plate electrostatic precipitator (ESP) is one of the most commonly applied particulate control devices to reduce fly ash emissions from utility boilers, incinerators, and many industrial processes. The design parameters have profound effects upon the precipitator performance. These include discharge wire diameter (dw), wire-to-wire distance (Sw-w), and plate-to-plate spacing (Sp-p).

Pontius and Sparks (1984) evaluated the performance of a pilot-scale ESP with different sizes of discharge electrodes. Their results showed that a significant improvement in the ESP performance could be achieved with large-diameter electrodes. But Abdel-Sattar (1991) pointed out that the precipitation efficiency increases with a decreasing discharge wire diameter.

* Corresponding author.

Hall (1984) demonstrated that an optimal value of the relative electrode spacing factor (Sw-w/Sp-p) exists and decreases with an increase of the duct width, thus yielding increased electric field strength at collecting surfaces even at a constant current density. Abdel-Sattar (1991) indicated that the plate-to-plate spacing, rather than the wire-to-wire distance, is the most effective parameter on the precipitator performance.

Wide duct technology is a new approach for the development of ESPs with high efficiency. The traditional plate spacing of an ESP is usually around 200 to 300 mm (Meyer-Schwinning 1984). However, there are numerous studies indicating the advantages of plate spacing as large as 600 mm. Chen and Wang (1984) employed 325 mm and 650 mm plate spacings in industrial performance tests. They indicated that advantages of a wide spacing ESP in comparison to the normal spacing one are low penetration rates and high energy savings. But for the plate spacing in the range of 250 to 500 mm, Darby (1984) indicated that the wide spacing ESP would lead to a high power consumption. Navarrete et al. (1997) showed that a wide plate spacing of 400 mm is a convenient device for the collection of high resistivity fly ash particles. An ESP with a plate spacing of 300 mm showed a better performance for the collection of low resistivity fly ash particles.

The performance of a wire plate ESP is usually obtained under different design criteria and operation indexes. This may be one of the reasons that different conclusions were made in the literature. As a result, similar improvements may not be obtained for other applications. The objective of this study is to employ a mathematical model to demonstrate the effects of some geometric parameters on the performance of a wire plate ESP operated at different operation indexes. The geometric design parameters being studied are the discharged wire diameter, the wire-to-wire distance, and the plate-to-plate spacing. And the operation indexes being evaluated are the electric field strength, the average current density at plates, and the corona power ratio.

DESCRIPTION OF MATHEMATICAL MODEL

Collection Efficiency

This model assumed that particles are well mixed by lateral turbulence in the gas stream (Licht 1988). As shown in Figure 1, the charging cell is divided into many small steps. The governing equation is given by

$$\eta_{i,j} = \frac{dn_{i,j}}{n_{i,j}} = \omega_{i,j}\frac{dt}{W/2} = \omega_{i,j}\frac{A_{c_j}}{Q}, \qquad (1)$$

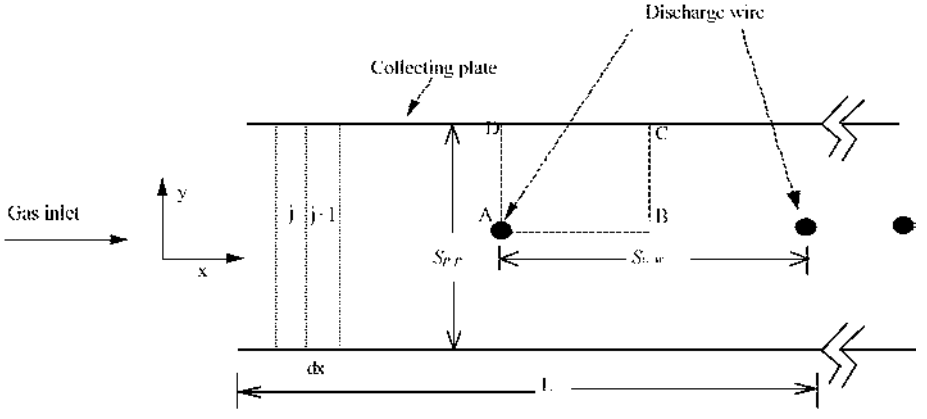

FIGURE 1. The computational domain of a wire plate ESP.

where $\eta_{i,j}$ is the collection fraction for the ith particle size in the jth increment length of an ESP; A_{C_j} is the collection plate area in the jth length increment; and $\omega_{i,j}$ is the migration velocity of the ith particle in the jth length increment. The overall grade efficiency is obtained from

$$\eta_{dp} = 1 - (1 - \eta_{i,1})(1 - \eta_{i,2}) \cdots \times (1 - \eta_{i,j-1})(1 - \eta_{i,j}) = 1 - \prod_{j=1}(1 - \eta_{i,j}). \quad (2)$$

The effective migration velocity ($\omega_{i,j}$) of a particle of diameter d_p is (Flagan and Seinfeld 1988)

$$\omega_{i,j} = q_{i,j} E_{p_j} C / 3\pi \mu d_p, \quad (3)$$

where $q_{i,j}$ is the charge on the particle in each j step; C is the Cunningham correction factor; μ is the gas viscosity; and E_{p_j} is the field strength on the plate.

The collecting field strength (E_{p_j}) and charge of the particle ($q_{i,j}$) are determined by electric state of an ESP and charging theory, respectively, as described in the following.

Electric State

The electric state of an ESP generally includes items such as the current–voltage relationship, the electric field, and the current density pattern in the interelectrode. They influence the electric field strength and the charging rate of particles. Main equations that govern the electric conditions in an ESP are the Poisson's equation and the current continuity equation (McLean 1988). The governing equations are

$$\nabla^2 V = -\frac{\rho_-}{\varepsilon_0}, \quad (4)$$

$$E = -\nabla V, \quad (5)$$

$$\nabla \cdot J = 0, \quad (6)$$

$$J = \rho_- b^- E, \quad (7)$$

where V is the voltage; ρ_- is the space charge density associated with ions generated by the central electrode; ε_0 is permittivity in a free space; E is the electric field; J is the current density; and b^- is ion mobility. And since the particulate mobility is several orders of magnitude less than the ionic mobility, only ionic current density appears in the current density Equation (6). McDonald et al. (1977) employed a finite difference method to solve the two-dimensional form of Equations (4)–(7). In this study, a similar approach is made to determine the electric state in the charging unit.

Boundary Conditions and Calculation Procedure

The boundary conditions for V in the computational domain shown in Figure 1 are written as

$$V = V_a \quad \text{at the wire,} \quad (8)$$

$$\rho_- = \rho_i \quad \text{at the wire,} \quad (9)$$

$$V = 0 \quad \text{along the collecting plate,} \quad (10)$$

$$\partial V / \partial y = 0 \quad \text{along the line AB,} \quad (11)$$

$$\partial V / \partial x = 0 \quad \text{along the lines AD and BC,} \quad (12)$$

where V_a is the applied voltage at the wire and ρ_i is the corona space charge density at the wire.

The calculation starts by solving the space charge free form of Equation (4). Then the entire charge density distribution is calculated from the current continuity Equation (6). The total current relation with charge density at the wire is given by

$$\rho_i = \frac{I_i / L_w}{2\pi b^- r_i E_i}, \quad (13)$$

where r_i is the radius of the ionized sheath; E_i is the electric field strength at the boundary of the ionized sheath; I_i is the corona current on the corona wire; and L_w is the length of the corona wire. The product $r_I E_i$ in Equation (13) can be determined by a common simplifying assumption (McDonald et al. 1977),

$$r_i E_i = a_c E_c \quad (14)$$

and E_c is the electric field strength at the surface of the corona wire,

$$E_c = 3 \times 10^6(\delta + 0.03(\delta/a_c)^{1/2}), \quad (15)$$

where δ is the relative density of air and a_c is the radius of a corona wire. Calculations of V and ρ_- are repeated at every grid point, and the potential at the wire is adjusted to meet convergence criteria. The convergence criteria are that the potential value at each grid point is within 0.1 V of its previous value and the total current density at the plate equals the given value of

$$\left|\frac{(J_p)_{given} - (J_p)_{calculated}}{(J_p)_{given}}\right| \leq 10^{-4}, \quad (16)$$

where

$$(J_p)_{given} = I_i/2LL_w, \quad (17)$$

where L is the length of the collection plate and $(J_p)_{calculated}$ is given by Equation (7).

The grid number in the numerical calculation is 21 × 21 in the cell for calculation. The ion mobility is determined by (Kallio 1987)

$$b^- = 1.768 \times 10^{-4}\left(\frac{T}{273}\right)^{1.51}\left(\frac{760}{P}\right) \text{ m}^2/\text{V s}. \quad (18)$$

The ion mobility equation given in Equation (18) was obtained from laboratory air experiments. Due to the limited information available, the effect of flue gas composition on this expression is unknown at the present time. It is assumed that Equation (18) can be applied to the flue gas condition.

Charging Theory

Particles in a corona field are charged simultaneously by both field and diffusion charge. Lawless and Altman (1994) combined the two charging rates for calculating the charge of particles:

- For $\upsilon < 3\psi$, where particles are in the field charging zone,

$$\frac{d\upsilon}{d\tau} = \frac{3\psi}{4}\left(1 - \frac{\upsilon}{3\psi}\right)^2 + f(\psi); \quad (19)$$

- and for $\upsilon \geq 3\psi$, where particles are in the diffusion charging zone,

$$\frac{d\upsilon}{d\tau} = f(\psi)\frac{(\upsilon - 3\psi)}{\exp(\upsilon - 3\psi) - 1} \quad (20)$$

and

$$\upsilon = \frac{qq_e}{2\pi\varepsilon_0 d_p kT}, \quad (21)$$

$$\psi = \frac{q_e d_p E}{2kT}, \quad (22)$$

$$\tau = \frac{\rho_-}{\varepsilon_0} b^- t, \quad (23)$$

$$f(\psi) = \sin\left(\arctan\left(\frac{1.13}{\psi^{1/2}}\right)\right), \quad (24)$$

where the value of 3ψ is commonly called the saturation charge of the field charge; q_e is the unit electron charge; k is the Boltzmann's constant; T is the absolute temperature; and t is the actual residence time. Lawless and Altman (1994) compared their results from Equations (19) and (20) to the experimental observations for particles in the size ranges from 0.1 to 20 μm, and the comparisons are in good agreement.

To calculate electric states at different locations, the above charging equations, (19) and (20), are modified as

$$\frac{dq}{dt} = \left(\frac{d\nu}{d\tau}\right) \times \left(\frac{\rho_-}{\varepsilon_o} b^-\right) \Big/ \left(\frac{q_e}{2\pi\varepsilon_0 d_p kT}\right). \quad (25)$$

The electric field (E) and space charge density (ρ_-) are changed as the particle path changes. Average values of space charge and field strength in each j length are used for calculating particle charge Equation (25). The fourth-order adaptive-step-size Runge–Kutta numerical method is employed, and the length of each j step is 10^{-6} m.

RESULTS AND DISCUSSION

Model Validation

The accuracy of the present model has been checked with the authors' experimental data (Chang and Bai 1999). It has also been checked with published results in the literature. Figures 2a and 2b shows a comparison of the model result with the experimental data of Kihm (1987) and Salcedo and Munz (1987). It is noted that these two experiments were conducted under different values of dw, Sw-w, and Sp-p, but both were under well-mixed flow conditions. It is seen that the predicted results are in good agreement with the experimental collection efficiencies in the literature.

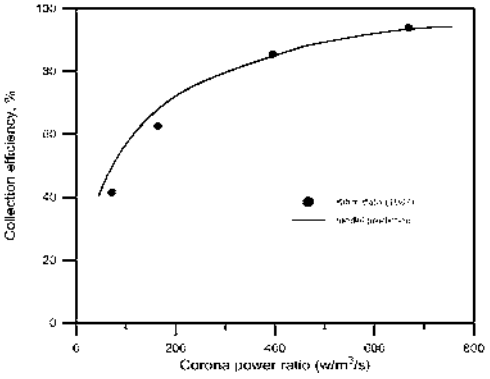

FIGURE 2a. Comparisons between the predicted collection efficiency and experimental data of Kihm (1987). (Experimental conditions in Kihm (1987): monodisperse inlet particle diameter = 4 ¹ m, duct spacing = 50 mm, wire-to-wire spacing = 50.8 mm, and wire diameter = 0.89 mm.)

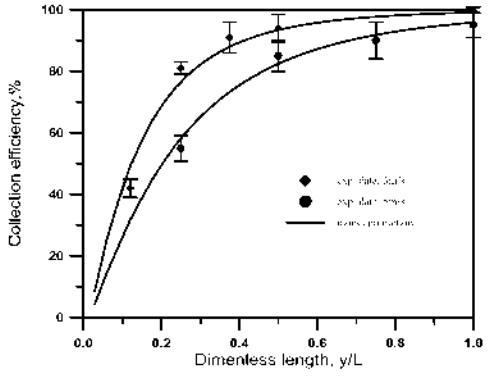

FIGURE 2b. Comparisons between the predicted collection efficiency and experimental data of Salcedo and Munz (1987). (Experimental conditions in Salcedo and Munz (1987): inlet particle MMD = 13.7 ¹ m, geometric standard deviation = 1.76, duct spacing = 162 mm, wire-to-wire spacing = 152 mm, wire diameter = 1.36 mm, and applied voltage = 38 kV.)

After validation of the model, it is used to evaluate the effect of each geometric design parameter on the ESP collection efficiency. Table 1 lists values of design and operation parameters for the model study. The parameter values cover the typical operation range of field ESPs. It is noted that the calculations were made based on holding the total ESP volume constant. Hence the specific collection area varies as the plate-to-plate spacing changes.

Effect of Discharge Wire Diameter

A constant (pseudo-homogenous) electric field strength (Eps) is used commonly as an operation index for the evaluation of an ESP performance. The definition of Eps is

$$Eps = \frac{Va}{0.5Sp - p}, \tag{26}$$

where Va is the applied voltage. Figure 3a shows the effect of discharge wire diameter on the particle penetration to the ESP as a function of electric field strength. The results indicated that a better collection is gained using a thin discharge wire under the same applied electric field strength (voltage) condition. For example, when operation parameter is at 3 kV/cm, the particle penetration rate is 3% with a wire diameter of 1 mm. It is less than the penetration rate of 13% as obtained by using discharge wires of 3 mm diameter. And the differences in the collection efficiency are significantly increased as the operation electric field strength is decreased.

Figure 3b shows the effect of discharge wire diameter on the particle penetration rate as a function of average current density at the collector plates. The average current density is usually used as an operation index if high resistivity

TABLE 1. Parameter values used in the study of ESP performance.[a]

		Range for Simulation	Base Case
Geometric parameter	Discharge wire diameter (dw)	1–3 mm	1 mm
	Wire-to-wire space (Sw-w)	60–360 mm	120 mm
	Plate-to-plate space (Sp-p)	100–600 mm	280 mm
Operation parameter	Electric field strength (Eps)	2–4 kV/cm	
	Average current density	0.1–3.5 mA/m^2	
	Corona power ratio	100–1000 Watts/m^3/s	

[a] The model study is performed at a constant temperature of 140°C with gas velocity of 1 m/s, a residence time of 3 s, an inlet particle mass median diameter of 10 μm, and a particle geometric standard deviation of 2.0.

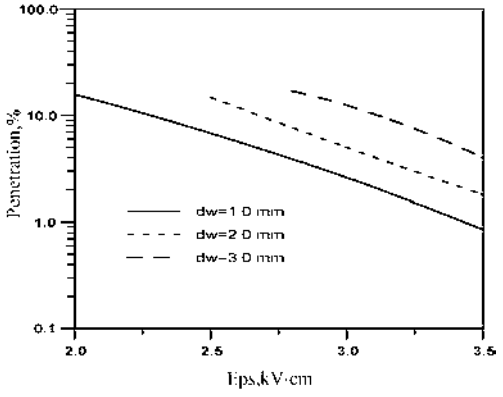

FIGURE 3a. The effect of discharge wire diameter on the ESP collection efficiency as a function of electric field strength. The particle space charge effect is neglected.

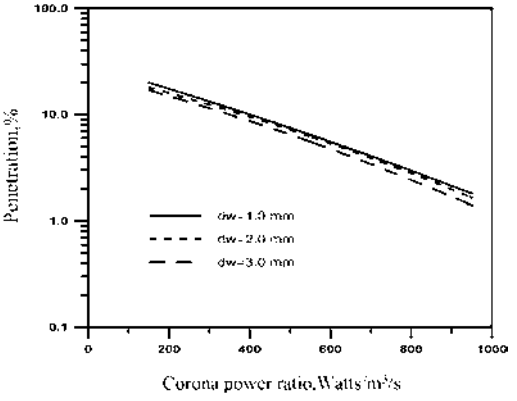

FIGURE 3c. The effect of discharge wire diameter on the ESP penetration as a function of corona power ratio. The particle space charge effect is neglected.

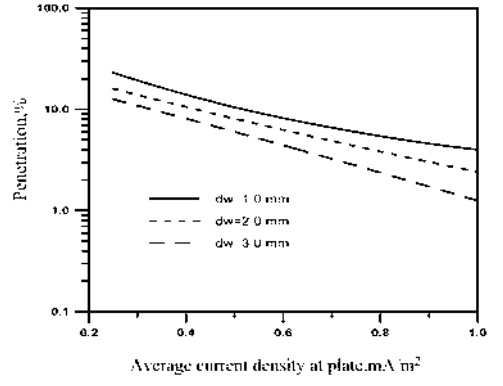

FIGURE 3b. The effect of discharge wire diameter on the ESP penetration as a function of average current density at collector plates. The particle space charge effect is neglected.

particles are of concern. This is because the ESP operation is limited by the allowable average current density at plates under this condition. An excessive operation over allowable current may lead to back corona. It is observed from Figure 3b that using discharge wires of a larger diameter tends to obtain a better collection than using thin wires.

The results shown in Figure 3b are opposite of those shown in Figure 3a as operating the ESP under a fixed applied voltage. This explains why different conclusions were obtained by Pontius and Sparks (1984) and Abdel-Satter (1991). The results of Pontius and Sparks (1984) were based on the same current limitation, while the conclusion of Abdel-Satter (1991) was made based on the applied voltage limitation.

The corona power is the main power consumption of the ESP system and is related to the ESP operation cost. Thus the corona power ratio is also a commonly used operation index. The definition of corona power ratio is total power over total flow rate, P/Q (Watts/m^3/s, $P = IV$). The effect of discharge wire diameter on the particle penetration rate as a function of corona power ratio is shown in Figure 3c. It is seen that an ESP with a smaller discharge wire diameter requires a higher power consumption to achieve the same penetration rate. But the difference in power consumption for different wire sizes to achieve the same penetration rate is not significant.

Effect of Wire-to-Wire Distance

Figure 4a shows the particle penetration rate of a wire-plate ESP as a function of electric field strength at various wire-to-wire spacing conditions. It seems that there is an optimal wire-to-wire distance for obtaining the best collection. For example, the best collection observed from Figure 4a is when using a 120 mm wire-to-wire spacing for an ESP operated below 3.5 kV/cm. But one can also see that the effect of wire-to-wire spacing is not significant when the electric field strength is used as the operation limitation; the differences in the EPS penetration between different wire-to-wire spacings are within 3%.

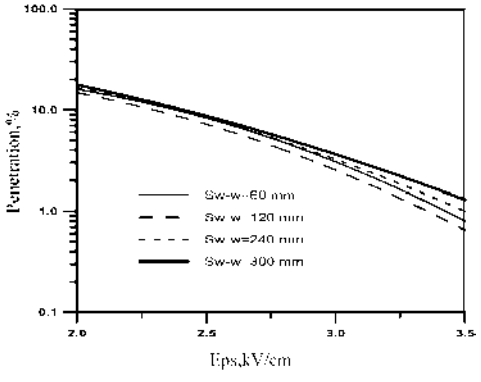

FIGURE 4a. The effect of wire-to-wire spacing on ESP penetration as a function of electric field strength. The particle space charge effect is neglected.

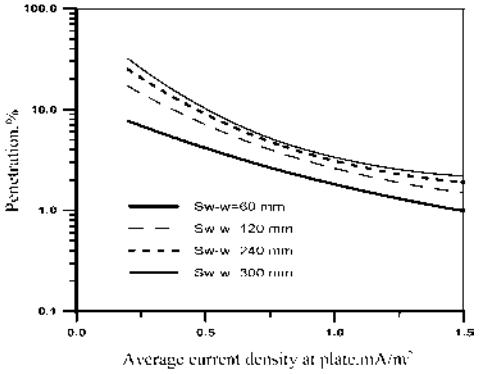

FIGURE 4b. The effect of wire-to-wire spacing on ESP penetration as a function of average current density. The particle space charge effect is neglected.

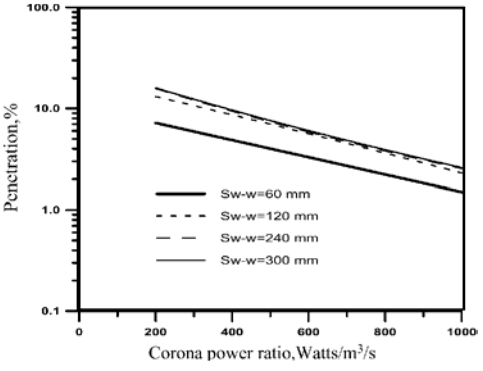

FIGURE 4c. The effect of wire-to-wire spacing on ESP penetration as a function of corona power ratio. The particle space charge effect is neglected.

Figure 4b shows the particle penetration rates as a function of average current density for different wire-to-wire spacings. As can be seen, a shorter wire-to-wire spacing applied to the system tends to achieve a better collection under the same average current density. For example, for wire-to-wire spacing decreases from 300 mm to 60 mm under the same current density of 0.5 mA/m^2, the decrease in the penetration rate is about 7%.

Figure 4c shows the relationship of corona power ratio with the penetration rate of a wire-plate ESP for different wire-to-wire spacings. It is observed that less penetration is obtained by a shorter wire-to-wire spacing ESP under the

same corona power ratio condition. The results also indicate that under the same design efficiency, an ESP with a larger wire-to-wire spacing requires more energy to keep its corona field. For example, for the same penetration rate of 5%, the power consumption for an ESP with 240 mm wires is doubled as compared to that with 60 mm wires.

Effect of Plate-to-Plate Spacing

It is usually considered that when the applied voltage is used as an operation reference, the penetration rate of an ESP is increased as the plate-to-plate spacing increases. This is because the electric field strength decreases significantly with increasing plate-to-plate spacing under the same applied voltage. However, recently there is also an indication of adopting wide plate ESPs to increase the collection efficiency (Darby 1984; Pontius and Sparks 1984; McLean 1988; Offen and Altman 1991; Grieco 1994). The wide spacing phenomena are usually referred to as "non-Deutschian phenomena."

The Eps is the most popular index to compare the performance of different duct widths. Figure 5a shows the penetration rate of a wire-plate ESP as a function of Eps under different duct widths. All the original dimensions of design are kept constant, except that duct width

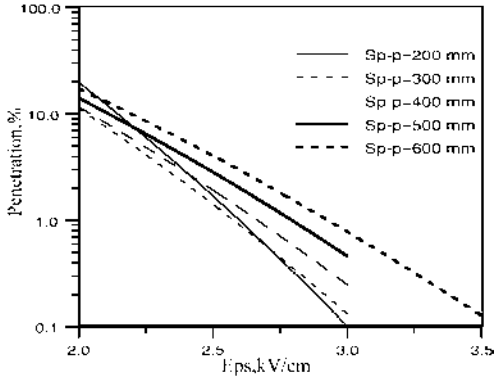

FIGURE 5a. The effect of plate spacing on the ESP penetration as a function of electric field strength. The particle space charge effect is neglected.

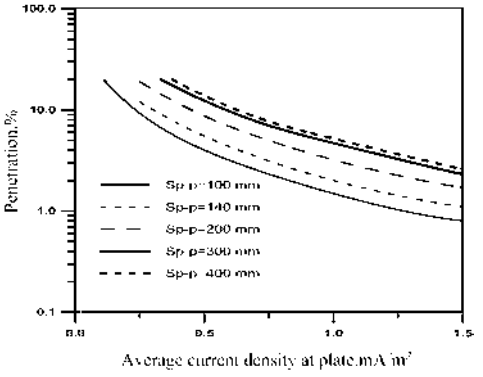

FIGURE 5b. The effect of plate spacing on the ESP penetration as a function of average current density. The particle space charge effect is neglected.

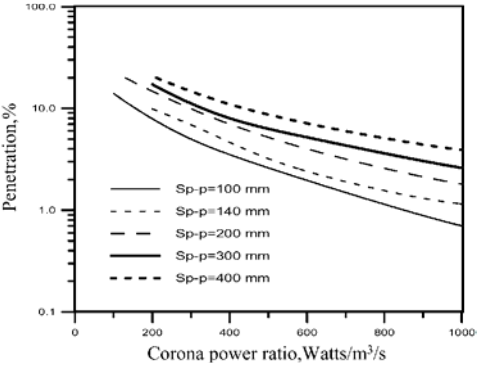

FIGURE 5c. The effect of plate spacing on the ESP penetration as a function of corona power ratio. The particle space charge effect is neglected.

is changed from 200 to 600 mm. It is seen in Figure 5a that the penetration rate does not have a regular trend with changes in the duct spacing. It seems that the optimal duct width changes as the value of Eps varies. For example, the penetration rate for an ESP with a 500 mm spacing is less than that with a 200 mm duct spacing at an Eps value of lower than 2.2 kV/cm. It appears that an ESP with 600 mm duct spacing tends to give the highest penetration under the value of Eps larger than 2.1 kV/cm.

Although the wide duct phenomena (with duct width larger than the traditional values of 200–250 mm) can be described partially as the comparison based on the same Eps, it has been

shown (Cheng and Wang 1984; Navarrete et al. 1997) that a wide duct ESP can usually be operated at a higher Eps than the traditional ESP. As a result, the optimal duct width in a real application may be increased to be wider than those predicted in Figure 5a.

Figure 5b shows the penetration rate of a wire-plate ESP as a function of average current density at plates for various duct spacing conditions. It is seen that the design of a narrow duct spacing tends to obtain less penetration than the design of a wide duct spacing under the same average current density at plate.

Figure 5c shows the relationship of particle penetration rate versus corona power ratio for different duct spacings. It is seen that high power consumption is required to reach the same penetration for an ESP with wide spacing. This is because the increase of duct spacing will consume more energy to keep the corona field. Besides, more energy is also consumed to enhance the particle migration velocity for compensation of the increase of transport path. As a result, although the configuration of wide spacing can save initial installation costs due to fewer plates and electrodes, the operation costs may increase due to high power consumption. For example, if the total effective width of the ESP is 4 m, the number of collection electrodes and discharge wires under a duct spacing of 400 mm could be saved up to 52% and 50%, respectively, as compared to those under a duct spacing of 200 mm (the plate thickness is neglected). But for reaching the same penetration of 5%, the corona power consumption for an ESP with a duct spacing of 400 mm is about 160% of that with 200 mm duct spacing. Similar observations can also be seen in Darby (1984). But results obtained by Chen and Wang (1984) were different in that they indicated a low energy cost for a wide spacing ESP. The reason for this is not clear at the present time.

Effect of Particle Characteristics

The conditions of sparking occurrence have not been clearly defined so far. However, Turner et al. (1988) provided a reasonable equation for estimating the sparking field strength (Es, V/m),

$$\mathrm{Es} = 6.3 \times 10^5 \times \left(\frac{273}{T} \times P\right)^{1.65}, \qquad (27)$$

where T is absolute temperature (K); and P is the gas pressure (atm). In practice, they noted that the electric field strength (Eps) must be controlled to be less than Es for avoiding excessive sparks.

On the other hand, if the particle resistivity is high, the allowable current density may be reduced. Figure 6 shows the interactions of sparking limitation with Eps of 3.0 kV/cm and current (back corona) limitations with maximum average current densities of 1.0 and 0.5 mA/m^2 for an ESP with 3 mm wire diameter. If the maximum average current density of a system can be operated at 1.0 mA/m^2, the collection efficiency is higher than that operated at 0.5 mA/m^2. However, this situation is impossible. This is because that sparking will occur before operating current reaches 1.0 mA/m^2. The maximum ESP efficiency is only around 92%. And if the allowable current density is reduced to 0.5 mA/m^2 due to a high particle resistivity, the interaction between back corona and sparking limitations

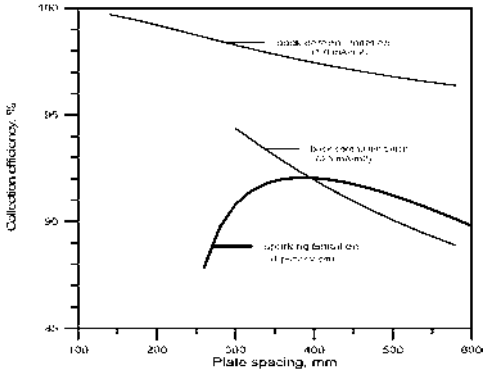

FIGURE 6. The interaction of sparking (occurs at Eps of 3 kV/cm) and back corona (occurs at average current densities of 0.5 and 1.0 mA/m2 at plates) limitations with 3 mm wire diameter. The dashed area indicates the operation limitation. The particle space charge effect is neglected.

occurs. This situation indicated that the collection efficiency is further reduced for plate spacing larger than 395 mm due to back corona. On the other hand, for duct width of less than 395 mm, a decrease in the duct width leads to a decrease in the ESP efficiency due to sparking limitation. Therefore the optimal plate spacing is around 395 mm for this case. This is wider than the traditional duct width of 200–300 mm. This may explain why some studies (Chen and Wang 1984; Navarrete et al. 1997) showed that the ESPs can be operated at less penetration with wider duct spacing.

The aforementioned results were obtained under conditions where the particle space charge effect was neglected. As the particle space charge effect is considered, Equation (4) becomes

$$\nabla^2 V = -\frac{\rho_- + \rho_P}{\varepsilon_0}, \qquad \textbf{(4a)}$$

where ρ_P is the particle space charge density.

Figure 7 shows the effect of discharge wire diameter on the ESP penetration as a function of electric field strength for a dust loading of 5 g/m^3, as compared to Figure 3a which is a similar plot but under the case of neglecting the particle space charge effect. The trend that less penetration is obtained using thin discharge wires under the same electric field strength is not biased. The difference between Figure 3a and Figure 7 is that the particle penetration for an ESP with thick wire diameter of 3 mm is higher if particle space charge effect is considered. But for an ESP with a thin wire diameter of 1 mm, the penetration rates are about the same no matter whether particle space charge is considered or not. We refer the reader to Chang (1998) for a detailed discussion of the effects of other particle characteristics (such as particle size distributions) on the ESP performance.

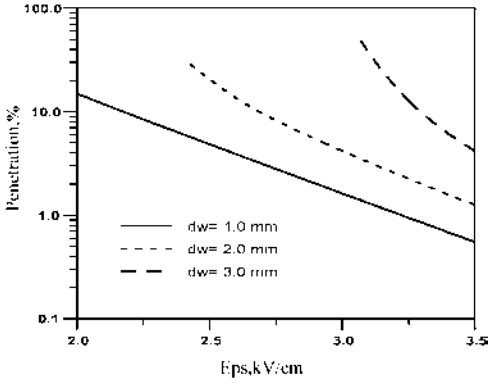

FIGURE 7. The effect of discharge wire diameter on the ESP penetration as a function of electric field strength. The particle space charge effect is considered under the inlet particle mass loading of 5 g/cm^3.

CONCLUSION

An evaluation of influences of some geometric design parameters on the ESP performance at three different operation indexes was presented in this study. The results demonstrated that the penetration rate is lower for an ESP with a thick wire size, a small wire-to-wire distance, and a narrow plate-to-plate spacing under the same average current density at plate condition. On the other hand, if the electric field strength is used as the comparison basis, the penetration rate is lower for a smaller wire diameter. And the influences of wire-to-wire spacing and plate-to-plate spacing on the ESP performance do not have regular trends. Optimal design values exist but they varied as the electric field strength changed.

The effect of particle space charge may be significant on the particle penetration rate for an ESP with thick discharge wires. But the penetration rates are almost the same whether particle space charge effect is considered or not for an ESP employing thin discharge wires. In addition, the particle space charge effect does not change the trend in the variation of particle penetration rate with the variation of values of design parameters as mentioned earlier.

References

Abdel-Sattar, S. (1991). Influences of Geometrical Parameters Upon Electrostatic Precipitator Efficiency, *Compel—The International J. for Comput. & Math. in Electrical & Electronic Engineering* 10:27–43.

Chang, C.-L. (1998). Influences of Design and Operation Parameters on the ESP Efficiency. Ph.D. Dissertation, National Chiao-Tung University, Hsinchu, Taiwan.

Chang, C.-L., and Bai, H. (1999). An Experimental Study on the Performance of a Single Discharge Wire-Plate Electrostatic Precipitator with Back Corona, *J. Aerosol Sci*. 30:325–340.

Chen, G. J., and Wang, L. Q. (1984). The Research and Application of Electrostatic Precipitator with Wide Spacing and Cross-Positioned Channel Collecting Plates in the Power Plant, *Proc. 2nd Inter. Conf. on Electrostatic Precipitation*, Kyoto, Japan, Air Pollution Control Assoc., pp. 362–367.

Darby, K. (1984). Plate Spacing Effect on Precipitator Performance, *Proc. 2nd Inter. Conf. on Electrostatic Precipitation*, Kyoto, Japan, Air Pollution Control Assoc., pp. 376–383.

Flagan, R. C., and Seinfeld, J. H. (1988). Fundamentals of Air Pollution Engineering, Prentice–Hall, NJ.

Grieco, G. J. (1994). Understand, Solve Problems with ESP Wide Plate Spacing, *Power* 138:43–48.

Hall, H. J. (1984). Some Electrode Geometry, Electric Field and Performance Effects in Electrostatic Precipitation, *Proc. 2nd Inter. Conf. on Electrostatic Precipitation*, Kyoto, Japan, Air Pollution Control Assoc., pp. 354–361.

Kallio, G. A. (1987). Interaction of Electrostatic and Fluid Dynamic Fields in Wire-Plate Precipitators. Ph.D. Dissertation Dept. of Mech. and Materials Engrg., Washington State University, Bellingham, Washington.

Kihm, K. D. (1987). Effect of Nonuniformities on Particle Transport in Electrostatic Precipitators. Ph.D. Thesis, Stanford University, Stanford, CA.

Lawless, P. A., and Altman, R. F. (1994). ESPM: An Advanced Electrostatic Precipitator Model, *IAS Annual Meeting (IEEE Industry Applications Society)*, 1519–1526.

Licht, W. (1988). *Air Pollution Control Engineering: Basic Calculations for Particulate Collection*, 2nd ed., Marcel Dekker, Inc., p. 107.

Meyer-Schwinning, G. (1984). The Increased Passage Width-Development Steps and Results Achieved with Industrial Installations, *Proc. 2nd Inter. Conf. on Electrostatic Precipitation*, Kyoto, Japan, Air Pollution Control Assoc., pp. 929–936.

McDonald, J. R., Smith, W. B., Spencer, III, H. W., and Sparks, L. E. (1977). A Mathematical Model for Calculating Electrical Conditions in Wire-Duct Electrostatic Precipitation Devices, *J. of Appl. Phys*. 48:2231–2243.

McLean, K. J. (1988). Electrostatic Precipitators, *IEE Proc*. 135:347–361.

Navarrete, B., Canadas, L., Cortes, V., Salvador, L., and Galindo, J . (1997). Influence of Plate Spacing and Ash Resistivity on the Efficiency of Electrostatic Precipitators, *J. of Electrostatics*. 39:65–81.

Offen, G. R., and Altman, R. F. (1991). Issues and Trends in Electrostatic Precipitation Technology for U. S. Utilities, *J. Air & Waste Manage. Assoc*. 41:222–227.

Pontius, D. H., and Sparks, L. E. (1984). Effect of Wire Diameter on Particle Charging and Collection Efficiency in Electrostatic Precipitators, *Proc. 2nd Inter. Conf. on Electrostatic Precipitation*, Kyoto, Japan, Air Pollution Control Assoc., pp. 269–274.

Salcedo, R., and Munz, R. J. (1978). The Effect of Particle Sharp on the Collection Efficiency of Laboratory-Scale Precipitators, *Proc. 3rd Inter. Conf. on Electrostatic Precipitation*, Abano-Padova, Italy, Air Pollution Control Assoc., pp. 343–359.

Turner, J. H., Lawless, P. A., Yamamoto, T., Coy, D. W., Greiner, G. P., McKenna, J. D., and Vatavuk, W. M. (1988). Sizing and Costing of Electrostatic Precipitators Part I. Sizing Consideration, *J. Air. Poll. Cont. Assoc*. 38:458–471.

Received October 26, 1998; accepted September 21, 1999.